(Received 26 November 2023, Accepted 27 January 2024, Scheduled 10 February 2024)

A Compact Coplanar Waveguide Spoof Surface Plasmon Polariton with Enhanced Field Confinements

Chao Pang and Lin Li*

School of Information Science and Engineering, Zhejiang Sci-Tech University, Hangzhou, Zhejiang, China

ABSTRACT: In this article, a spoof surface plasmon polariton (SSPP) based on coplanar waveguide (CPW) with flipper structures is proposed to improve field confinement. The analyses based on the developed equivalent circuit (E.C) reveal that the proposed unit exhibits flexibly controllable dispersion features and improved field confinements owing to the introduction of the flipper structures. Finally, the proposed SSPP TL is designed, fabricated, and tested to validate the design principles. The experiment results illustrate the theoretical analyses and validate that the proposed SSPP TL exhibits ultra-compact size occupation and enhanced field confinement.

1. INTRODUCTION

The concept of spoof surface plasmon polarization (SSPP) is developed to mimic natural SPPs at terahertz and microwave frequencies [1]. Different structures such as one-dimensional arrays of grooves have been employed to construct SSPP transmission lines (TLs) [2–6]. However, if stronger field confinement in the millimeter or microwave band is expected, deeper grooves and hence a geometrical size are required which poses a crucial limitation for many real applications.

To break through this restriction, many compact SSPPs with strong field confinements are reported in recent years. In [7], a novel SSPP TL with zigzag grooves is proposed. By using such grooves, the SSPP TL can exhibit ultra strong field confinement with a limited strip width. Capacitive loading techniques are utilized in [8, 9] to manipulate the dispersion characteristics and enhance field confinement. In [10], an on-chip SSPP TL with reduced size and ultra-strong field confinement using 0.18 µm Complementary Metal Oxide Semiconductor (CMOS) technology is proposed. However, relatively complicated mode-conversion structures are still required to convert guided waves to SSPP wave [7–10], increasing transversal width largely. In [11–13], three advanced SSPPs with enhanced field confinement are reported. In [14], a new coplanar waveguide (CPW) SSPP with a simple and efficient mode-conversion transition structure is proposed, exhibiting the advantages of lower cut-off frequency (8.9 GHz) and stronger field confinement than the conventional CPW SSPP. Based on the CPW SSPP in [15], we proposed another new SSPP with improved field confinement. However, field confinements of these SSPPs are still not strong enough.

In this work, a novel CPW SSPP TL with flipper structures is proposed. Dispersion analyses based on the equivalent circuit reveal the stronger confinement ability of this new TL than conventional unloaded one. Measured S-parameters and simulated electric field distributions indicate enhanced field confinement ability due to the introduced flipper structure. Finally, experimental example is designed and fabricated to validate our design principles. The experimental results are in accordance with the theoretical ones. The ultra-strong field confinement of the proposed spoof SPP TL can be utilized to suppress the crosstalk or reduce the area of some microwave devices.

2. THEORY AND DESIGN PRINCIPLE

In our previous work [15], we proposed a CPW SSPP TL with stepped groove structures. Based on that SSPP, we designed a new CPW SSPP unit by loading flipper structures as shown in Figure 1. The material of the substrate in Figure 1 and all the following examples in this paper is FR4 with a dielectric constant of 4.4, a loss tangent of 0.02, and a thickness of 0.8 mm.

As shown in Figure 1, The proposed unit consists of a central CPW line with the line width of w_m and coupled gap of w_p. The parameter p denotes the period of the unit cell. Each stepped groove structure is composed of one wider slot line with the width of w_{s1} and length of l_{s1}, and one narrower slot line with the width of w_{s2} and length of l_{s2}. The flipper structure consists of a metallic patch with the width of w_1 and length of l_1 on the bottom layer of the unit. The metallic patch is connected to the CPW ground on the top layer through a metallic via with the radius of d.

To further explain operating principle of the proposed SSPP TL unit cell, we developed an equivalent circuit (E.C) model in Figure 1 according to the coupled-mode theory [16]. In the E.C model, the two capacitors C represent the effect of the flipper structures. The two TL models (Z_s, θ_s) represent the two CPW lines with the width of w_s and length of $p/2$. The TL models (Z_1, θ_1) and (Z_2, θ_2) represent the wider and narrower slot lines in each stepped groove structure, respectively. The transformers represent the electromagnetic coupling between the etched groove structures and the CPW line. Obviously, the unloaded SSPP corresponds to the case that $C = 0$ [10].

* Corresponding author: Lin Li (lilin_door@hotmail.com).

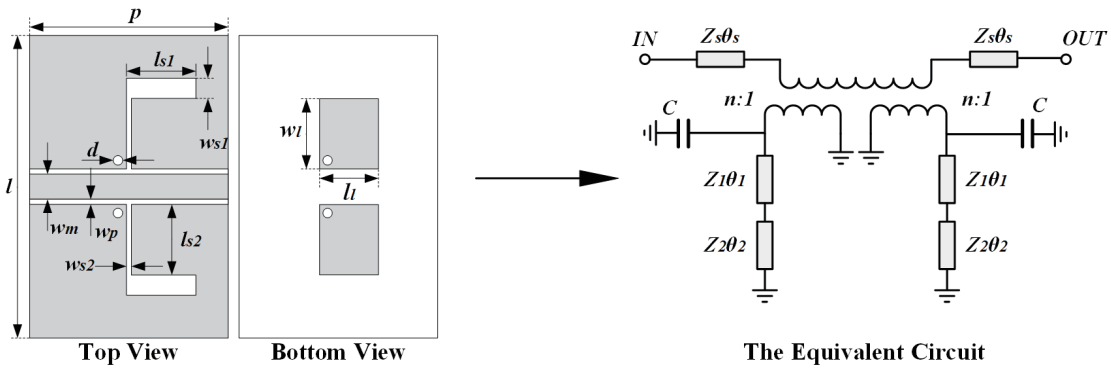

FIGURE 1. The proposed SSPP TL unit cell and its equivalent circuit.

In the E.C model, voltage and current on both sides of N_{th} unit cell (V_n, I_n, V_{n+1}, I_{n+1}) can be connected by transfer matrix which is also called $ABCD$ matrix as follows:

$$\begin{bmatrix} V_n \\ I_n \end{bmatrix} = \begin{bmatrix} A & B \\ C & D \end{bmatrix} \begin{bmatrix} V_{n+1} \\ -I_{n+1} \end{bmatrix} \tag{1}$$

where A, B, C, and D represent the parameters of the $ABCD$ matrix. As a symmetric network ($A = D$), the propagation constant β should be in conformity with the subsequent relation:

$$\cos(\beta p) = A \tag{2}$$

By considering and combining Equations (2) and (3), then we can obtain the following relationship.

$$\beta = \cos^{-1}(A) = \cos^{-1}(\chi_1 + \chi_2 + \chi_3) \tag{3}$$

where:

$$\chi_1 = \frac{C\omega Z_1 \sin(2\theta_s)(Z_1 \tan\theta_1 + Z_2 \tan\theta_2)}{4n^2 Z_s [Z_1 (Z_1 \tan\theta_1 + Z_2 \tan\theta_2) + C\omega (Z_1 - Z_2 \tan\theta_1 \tan\theta_2)]} \tag{4}$$

$$\chi_2 = \frac{-Z_1 \cos(2\theta_s)(Z_1 \tan\theta_1 + Z_2 \tan\theta_2)}{Z_1 (Z_1 \tan\theta_1 + Z_2 \tan\theta_2) + C\omega (Z_1 - Z_2 \tan\theta_1 \tan\theta_2)} \tag{5}$$

$$\chi_3 = \frac{C\omega \cos(2\theta_s)(Z_2 \tan\theta_1 \tan\theta_2 - Z_1)}{Z_1 (Z_1 \tan\theta_1 + Z_2 \tan\theta_2) + C\omega (Z_1 - Z_2 \tan\theta_1 \tan\theta_2)} \tag{6}$$

It can be observed from Equation (3) that the value of C brought by the flipper structures influences the dispersion feature of the proposed unit. To further investigate the relationship between the asymptotic frequency and the dimension of loaded flipper structures, Figures 2(a) and (b) plot the E.C computed and electromagnetic (EM) simulated dispersion curves of the proposed unit for various l_1 and w_1, respectively. The dimension parameters in Figure 4 are set as follows: $w_{s1} = 2$, $w_{s2} = 0.15$, $l_{s1} = l_{s2} = 7$, $l_{s3} = 1.5$, $w_m = 2.45$, $w_p = 0.14$, $d = 0.2$, $l = 40$, and $p = 10$ (all dimensions are in mm).

As shown in Figure 2, the loaded unit cell exhibits typical SSPP response which remains near the air line at low frequencies but goes away at high frequencies. It can also be observed that the E.C computed results are in accordance with the EM results, which demonstrates the accuracy of the proposed E.C model. Figure 2(a) compares the dispersion curves when w_1 is fixed at 7 mm, but l_1 is different. It can be observed that the larger the value of l_1 is, the larger the capacitance introduced by the flipper structures is, and the lower the asymptotic frequency is. Also, Figure 2(b) discusses the dispersion features when l_1 is fixed at 8 mm, but w_1 is different. The larger value of w_1 achieves larger capacitance and thus results in lower asymptotic frequency.

In summary, since the difference between the loaded and unloaded unit is the introduction of extra flipper structures, the decrease in asymptotic frequency can be attributed to the capacitance brought by the extra flipper structures. Secondly, the larger the area of the metallic patch of the flipper structures ($l_1 \times w_1$) is, the larger the capacitance introduced by the flipper structures is, the lower the asymptotic frequency of the unit is. Since the decrease of the asymptotic frequency leads to the tighter field confinement, the proposed SSPP has stronger field confinement than conventional unloaded one. Moreover, the field confinement can be flexibly controlled by changing the geometrical dimension of the flipper structure without requiring modifications of the transversal geometrical configurations.

3. DESIGN AND MEASUREMENT

The unloaded and loaded SSPP TL based on the proposed unit is shown in Figures 3(a) and (b), respectively. It can be observed that these SSPP TLs consist of three different kinds of parts marked as I, II, and III, respectively. Part I is CPW region at two terminals. The dimensions of CPW are chosen so as to obtain an impedance of 50 Ω. Part II is the transition region working as a mode converter and an impedance transformer to

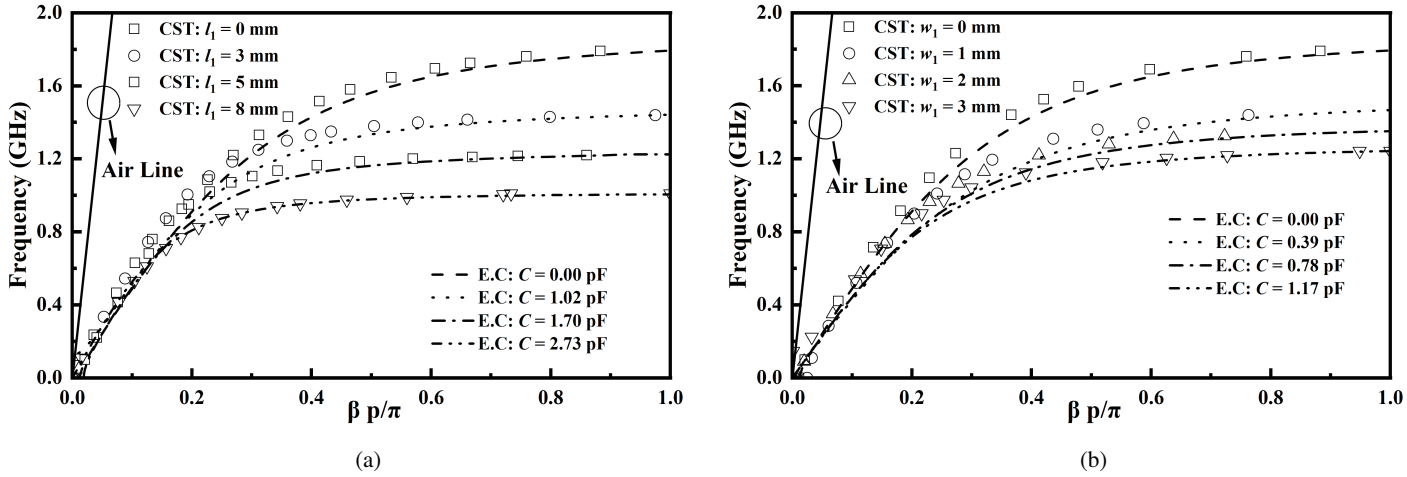

FIGURE 2. The dispersion curve with (a) fixed w_1 and different l_1 (b) different w_1 and fixed l_1.

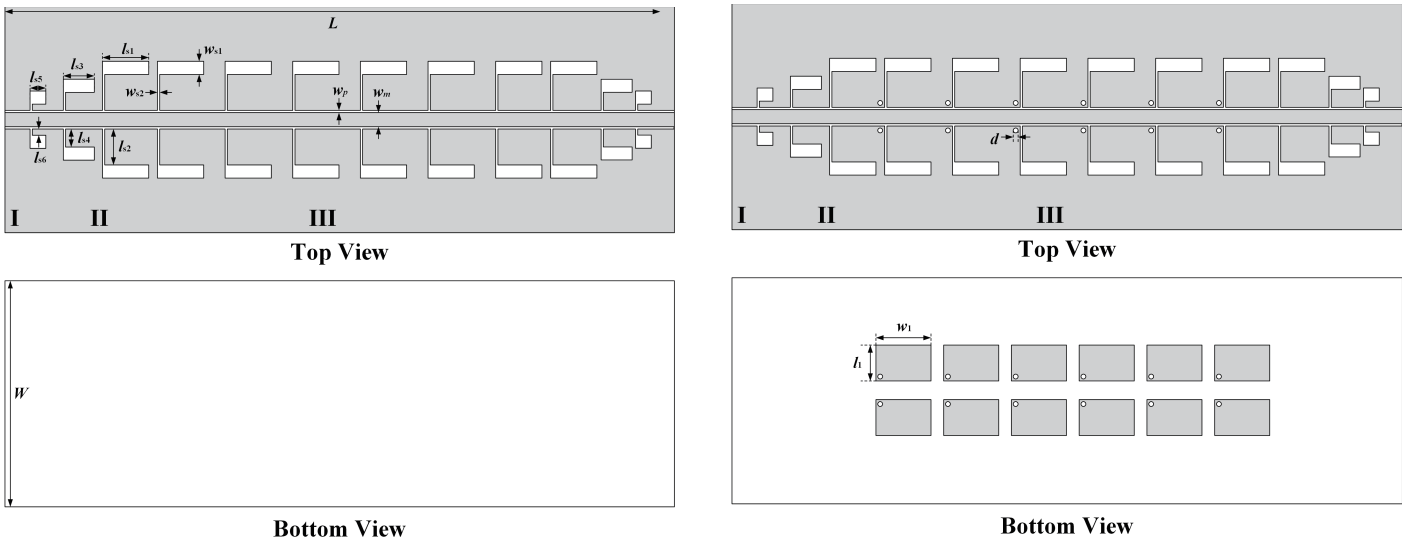

FIGURE 3. The layout of the (a) convention SSPP TL. (b) designed SSPP TL.

connect Part I and Part III. Part III is the SSPP transmission waveguide. The dimension parameters of the conventional and designed SSPP TLs are set as follows: $l_{s1} = l_{s2} = 7$, $w_{s1} = 2$, $w_{s2} = 0.15$, $w_m = 2.45$, $w_p = 0.14$, $d = 0.2$, $w_1 = 8$, $l_1 = 7$, $L = 100$, $W = 60$ (all dimensions are in mm).

To validate the lower asymptotic frequency of the proposed SSPP TL, Figure 4 compares the simulated S-parameters between the conventional and proposed SSPP TLs. It can be observed that the asymptotic frequencies of the conventional and proposed SSPP TL are 1.83 GHz and 0.94 GHz, which indicates that the designed SSPP TL exhibits stronger field confinements.

In order to visualize such strong field confinements, Figure 5 plots the normalized field distribution of the unloaded and loaded SSPP TL on the same cross section (x-z plane) at 1 GHz, respectively. It can be observed that the field is confined tighter near the designed SSPP TL than the conventional one. In addition, if the confinement region is defined as from the maximum electric field strength to 1/e, then the confinement region is reduced by about 37.82% from 3.94 mm to 2.45 mm, which indicates that the designed SSPP TL exhibits stronger field confinements.

We also fabricated the designed SSPP TL, and its top and bottom views are shown in Figures 6(a) and (b), respectively. Figure 7 depicts the measured and simulated S-parameters. It can be easily observed that the measured results are in accordance with the simulated ones, and the -3 dB asymptotic frequency is only 0.95 GHz, implying its ultra strong ability of field confinement. The fabrication tolerance and measurement environment are the main causes of the disparity.

It should also be noticed that the size of the proposed SSPP TL unit cell is only 10 mm$\times$20.93 mm, corresponding to 0.0021 λ_a^2 ($0.032\lambda_a \times 0.066\lambda_a$), where λ_a is the free space wavelength at the asymptotic frequency. For comparison, performances of the proposed SSPP TL and some previous SSPP TLs are listed

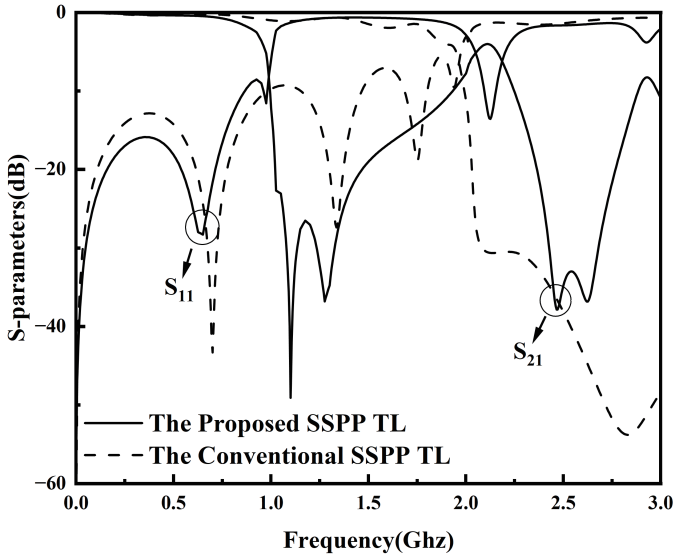

FIGURE 4. The simulated S-parameters comparison between the conventional and proposed SSPP TLs.

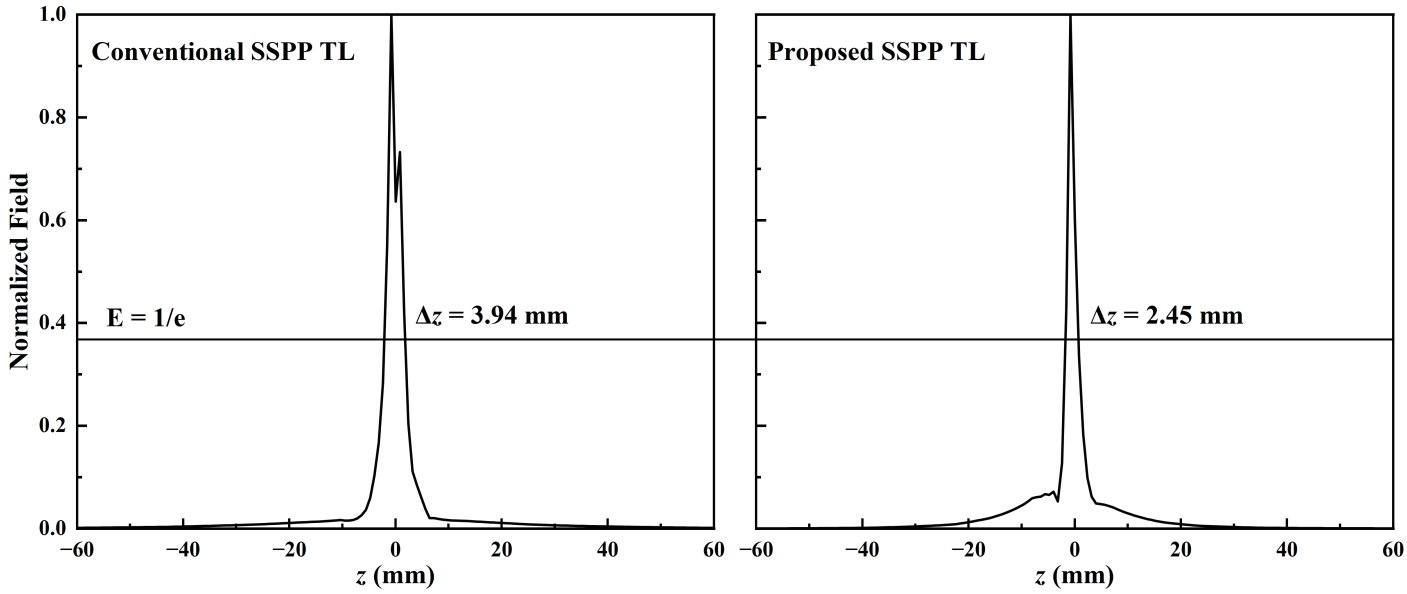

FIGURE 5. The normalized electric field of conventional and proposed SSPP TL.

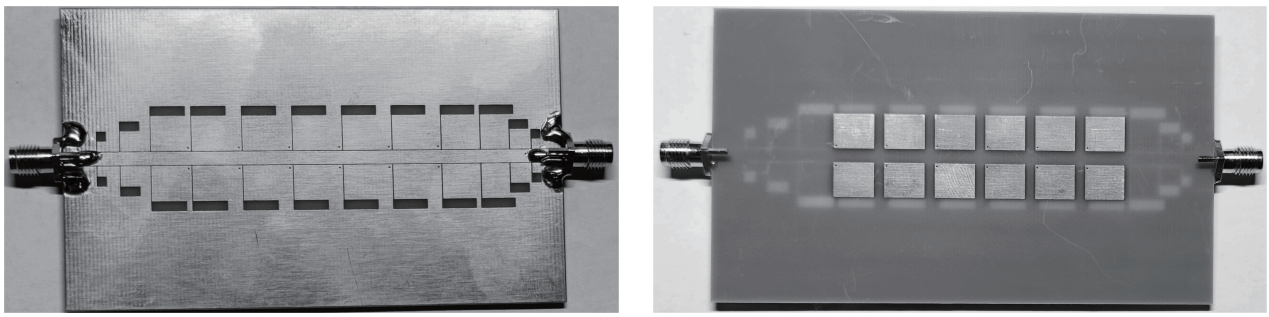

(a) (b)

FIGURE 6. The view of the fabricated SSPP TL from (a) top view. (b) bottom view.

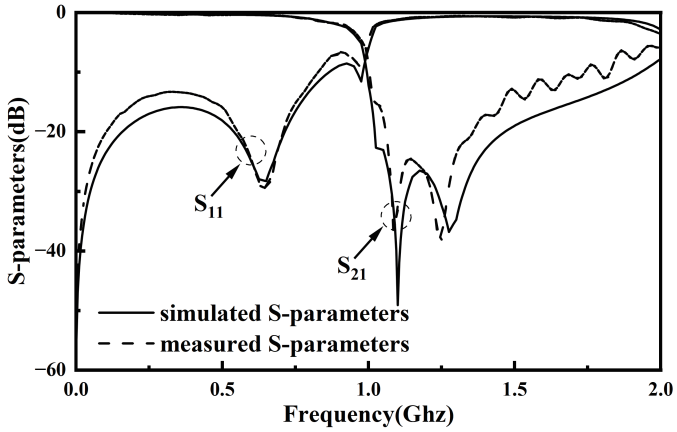

FIGURE 7. Simulated and measured S-parameters.

TABLE 1. Size performance of previous works and this work.

Ref.	f_a (GHz)	*unit size* (λ_a^2)	*overall size* (λ_a^2)
6	8.1	0.015 (0.14 × 0.11)	6.502 (5.40 × 1.20)
7	5.8	0.010 (0.10 × 0.10)	N.A.
12	8.9	0.019 (0.12 × 0.16)	0.418 (2.61 × 0.16)
13	1.67	0.007 (0.06 × 0.11)	0.042 (0.38 × 0.11)
This work	**0.95**	**0.002** (0.03 × 0.07)	**0.022** (0.32 × 0.7)

f_a: the asymptotic frequency, λ_a: the wavelength at f_a.

in Table 1 in terms of asymptotic frequency f_a, unit size, and overall size. It can be observed that the proposed SSPP TL exhibits more compact unit size and overall size.

4. CONCLUSION

In this article, a novel CPW SSPP TL is proposed. The analyses based on the E.C model reveal that the loaded SSPP exhibits a lower asymptotic frequency and tighter field confinement due to the capacitance brought by the extra flipper structures. It is also found that the field confinement of the loaded unit can be flexibly controlled. The experimental results and theoretical analyses agree well and validate that the loaded SSPP TL exhibits stronger filed confinements.

REFERENCES

[1] Barnes, W. L., A. Dereux, and T. W. Ebbesen, "Surface plasmon subwavelength optics," *Nature*, Vol. 424, No. 6950, 824–830, Aug. 2003.

[2] Gao, X. and T. J. Cui, "Spoof surface plasmon polaritons supported by ultrathin corrugated metal strip and their applications," *Nanotechnology Reviews*, Vol. 4, No. 3, 239–258, Jun. 2015.

[3] Zhang, D., K. Zhang, Q. Wu, R. Dai, and X. Sha, "Broadband high-order mode of spoof surface plasmon polaritons supported by compact complementary structure with high efficiency," *Optics Letters*, Vol. 43, No. 13, 3176–3179, Jul. 2018.

[4] Guo, Y.-J., K.-D. Xu, X. Deng, X. Cheng, and Q. Chen, "Millimeter-wave on-chip bandpass filter based on spoof surface plasmon polaritons," *IEEE Electron Device Letters*, Vol. 41, No. 8, 1165–1168, Aug. 2020.

[5] Xu, H., W.-S. Zhao, D.-W. Wang, and J. Liu, "Compact folded sspp transmission line and its applications in low-pass filters," *IEEE Photonics Technology Letters*, Vol. 34, No. 11, 591–594, Jun. 2022.

[6] Xu, J., Z. Li, L. Liu, C. Chen, B. Xu, P. Ning, and C. Gu, "Low-pass plasmonic filter and its miniaturization based on spoof surface plasmon polaritons," *Optics Communications*, Vol. 372, 155–159, Aug. 2016.

[7] He, P. H., H. C. Zhang, X. Gao, L. Y. Niu, W. X. Tang, J. Lu, L. P. Zhang, and T. J. Cui, "A novel spoof surface plasmon polariton structure to reach ultra-strong field confinements," *Opto-Electronic Advances*, Vol. 2, No. 6, 190001, 2019.

[8] Shi, Z., Y. Shen, and S. Hu, "Spoof surface plasmon polariton transmission line with reduced line-width and enhanced field confinement," *International Journal of RF and Microwave Computer-Aided Engineering*, Vol. 30, No. 8, e22276, Aug. 2020.

[9] Tang, X.-L., Q. Zhang, S. Hu, A. Kandwal, T. Guo, and Y. Chen, "Capacitor-loaded spoof surface plasmon for flexible dispersion control and high-selectivity filtering," *IEEE Microwave and Wireless Components Letters*, Vol. 27, No. 9, 806–808, Sep. 2017.

[10] He, P. H., D. Yao, H. C. Zhang, J. Wang, D. Bao, and T. J. Cui, "Ultra-compact on-chip spoof surface plasmon polariton transmission lines with enhanced field confinements," *Journal of Physics: Photonics*, Vol. 4, No. 4, Oct. 2022.

[11] Pan, H., B.-x. Li, and H. F. Zhang, "Anapole-excited terahertz multifunctional spoof surface plasmon polariton directional janus metastructures," *Physical Chemistry Chemical Physics*, Vol. 25, No. 16, 11 375–11 386, Apr. 2023.

[12] Guo, Z.-H., C.-J. Gao, and H.-F. Zhang, "Direction-dependent janus metasurface supported by waveguide structure with spoof surface plasmon polariton modes," *Advanced Materials Technologies*, Vol. 8, No. 2, 2200435, Jan. 2023.

[13] Li, Q.-Q. and H.-F. Zhang, "A high gain circularly polarized 2×2 antenna array based on the spoof surface plasmon polariton and spoof localized surface plasmon," *Journal of Electromagnetic Waves and Applications*, Vol. 37, No. 15, 1298–1316, Oct. 2023.

[14] Li, J., J. Shi, K.-D. Xu, Y.-J. Guo, A. Zhang, and Q. Chen, "Spoof surface plasmon polaritons developed from coplanar waveguides in microwave frequencies," *IEEE Photonics Technology Letters*, Vol. 32, No. 22, 1431–1434, Nov. 2020.

[15] Pang, C., R.-F. Cao, L. Li, and H.-W. Liu, "Spoof surface plasmon polariton based on stepped grooves and its application in compact low-pass filter design," *Plasmonics*, 2023.

[16] Ma, A., Y. Li, and X. Zhang, "Coupled mode theory for surface plasmon polariton waveguides," *Plasmonics*, Vol. 8, No. 2, 769–777, Jun. 2013.